

## 6 Flow over a Horizontal and Slightly Inclined Surfaces

In this chapter, an analysis of free convection fluid flow characteristics above a flat heated surface, which is placed horizontally and at small inclinations has been presented. The influence of inclination angles of the plate and heat fluxes on the flow characteristics has been reported. Three different flow patterns - attached, transition and buoyant plume which formed over the plate are discussed.

### 6.1 Theoretical analysis

Figure 6.1 depicts the free convection VBL over a slightly inclined flat plate ( $0^\circ \leq \phi \leq 10^\circ$ ) with a physical coordinate system. In the present work, a plate of length  $L = 150$  mm inclined at an angle of  $\phi$  and exposed to a constant wall heat flux  $q_w''$  has been considered. As indicated in figure 6.1, the left and right plate edges have been termed as the leading and trailing edges of the plate, respectively. The origin  $O$  is assumed to be located at the leading edge of the plate. The  $x$  and  $y$  coordinates represent the streamwise distance along the plate from the leading edge and the normal distance from the plate, respectively. In addition, the parallel and perpendicular components of velocity have been denoted as  $u$  and  $v$ , respectively. The forces of gravity ( $G$ ) and buoyancy ( $B$ ) act vertically downward and upward, respectively. Therefore, the components of buoyancy force parallel and perpendicular to the plate are  $B_x = B \sin \phi$  and  $B_y = B \cos \phi$ . Similarly,  $G_x = G \sin \phi$  and  $G_y = G \cos \phi$  are the gravitational force acting on the fluid element.

The relation between buoyancy and viscous forces is defined by Grashof number in free convection. The product of Grashof number and Prandtl number is the Rayleigh number. For a constant heat flux condition, the modified Rayleigh number is used. In the present work, the average modified Rayleigh number is defined as  $Ra_L^* = \frac{g\beta q_w'' L^4}{\alpha \nu k}$  where  $g$  the gravitational acceleration,  $L$  the length of the plate,  $q_w''$  the wall heat flux,  $\beta$  the thermal

expansion coefficient,  $\alpha$  the thermal diffusivity,  $\nu$  the kinematic viscosity, and  $k$  the thermal conductivity of water.

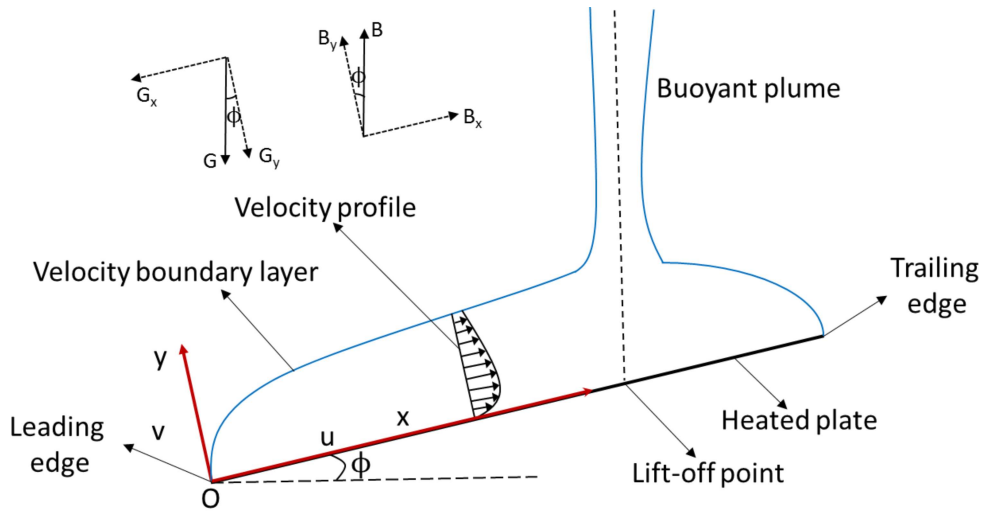


**Figure 6.1:** Physical configuration of slightly inclined horizontal plate

## 6.2 Experimental Details

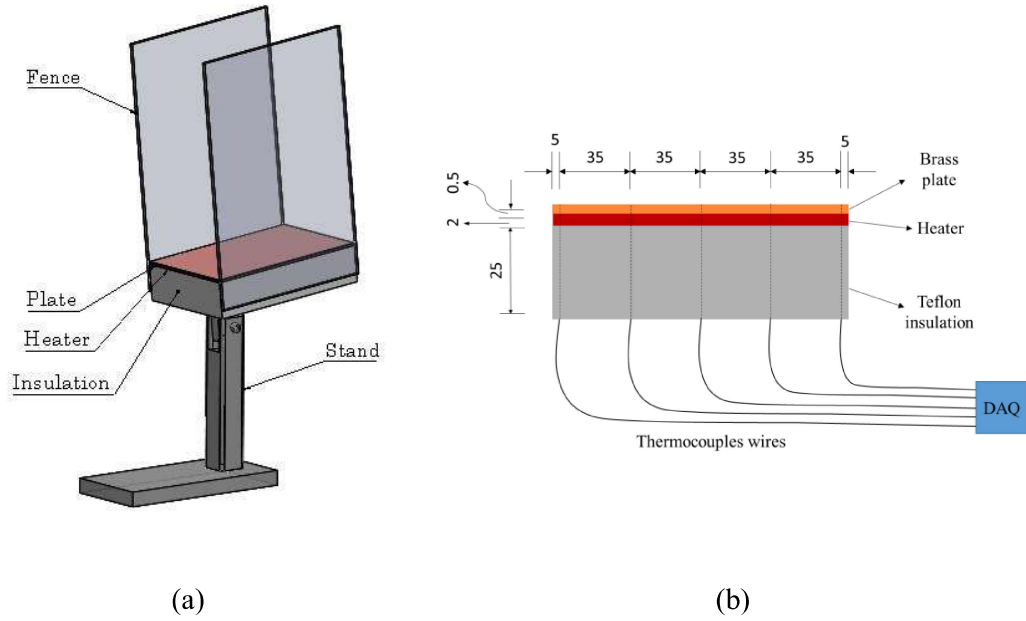
Figure 6.2(a) depicts a schematic representation of the flat plate assembly. A brass plate measuring 150 mm long, 100 mm wide and 0.5 mm thick was employed as the heating surface in the experiment. The plate was heated with a silicon rubber heater attached to its back side. To minimise heat loss from the back side of the heater, a 25 mm thick thermal insulation has been provided. The front surface of the plate was spray-painted with matte black to reduce surface reflection during the experiments [91]. This is essential when using a laser sheet for near wall measurements using PIV. To maintain a 2-D flow over the plate, the spanwise flow was restricted by using two fences of height 200 mm, fastened to either side of the plate assembly, as shown in figure 6.2(a). An arrangement for providing inclination to the plate assembly was also fabricated.

The position of the thermocouples used for the measurement of the plate surface temperature is shown in figure 6.2(b). K-type thermocouples with a 0.5 mm diameter were used to record the temperature of the surface of the plate. The thermocouples were inserted

from the backside of plate heater arrangement, and their tips are precisely aligned with the front surface of the plate. This configuration ensures that the thermocouples reliably detect the surface temperature while not interfering with the flow over the plate. The thermocouples are positioned in the centre of the plate at  $x = 5, 40, 75, 110,$  and  $145$  mm, as indicated in figure 6.2(b).

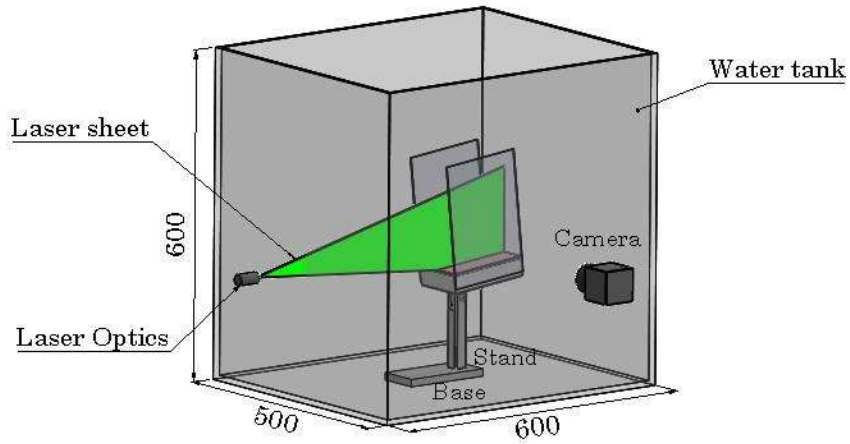
The flow structure that needs to be analysed in the current work develops close to the heated inclined plate. Therefore, the inclined plate assembly with the glass tank is intended to provide unrestricted free convection behaviour. This has been ensured by using a tank size which provides sufficient water depth and height below and above the plate respectively. As shown in figure 6.3, the plate assembly was placed in a glass tank that measured  $600 \times 600 \times 500$  mm. The minimum vertical distance between the trailing edge of plate and free surface of water obtained for a  $10^\circ$  inclined plate is 280 mm. The mean values of three thermocouples placed at distinct locations in the water tank were used to calculate the bulk temperature. A DAQ system was used to record the thermocouple values. The bulk water temperature used for the experiment is maintained at  $23 \pm 0.1$  °C. The laboratory temperature was also kept constant throughout the experiment at about 23 °C to reduce the effect of stratification. To minimize the effects of disturbance from the free surface of the water, a 20 mm thick thermocal sheet was placed on top of the tank. The experiment was performed at an inclinations angle of  $0^\circ, 2.5^\circ, 5^\circ, 7.5^\circ$  and  $10^\circ$  from horizontal and at three different heat fluxes of 500, 1000 and 2000 W/m<sup>2</sup>.

Figure 6.3 depicts the camera and laser sheet arrangement in relation to the slightly inclined plate assembly. PIV setup is explained in section 4.2.2, and the PIV recording parameter is also illustrated in Table 5.1.



All dimensions are in mm

**Figure 6.2:** (a) Schematics diagram of flat plate assembly and (b) Location of thermocouples used for the measurement of surface temperature



All dimensions are in mm

**Figure 6.3:** Schematic diagram of the experimental setup with camera and laser sheet position

### 6.3 Results and discussion

The objective of the present investigation is to study the flow characteristics over a horizontal and slightly inclined flat plate by PIV technique. In this section, flow structures have been analysed with the help of velocity contours and streamlines. After that, complete flow pattern for case of a horizontal plate has been discussed. Based on its results, the effect of a slight inclination and varying heat flux on the flow pattern is subsequently presented.

#### 6.3.1 Velocity contours and streamlines

In this section, streamlines and velocity contours have been used to illustrate the flow structure over different inclinations of the plate. Figure 6.4 shows the R-velocity ( $R = \sqrt{u^2 + v^2}$ ) contour and streamlines for plate inclination varying from  $0^\circ$  to  $10^\circ$  from horizontal at a heat flux of  $1000 \text{ W/m}^2$ . Three distinct flow patterns are discernible in all the figures. They are - (i) laminar flow (regime A) (ii) transition flow (regime B) and (iii) plume (regime C). For the case of the horizontal plate, it is seen that in the laminar regime, the fluid close to the surface flows from both ends of the plate towards the centre. As a result, a BL forms on either side of the heated plate. After some distance, the laminar flow gets transformed into transitional flow which is manifested by an increase in VBL thickness and increase in u-velocity. Finally, a plume rises from the far end of the transition region. When the plates are inclined, the position of these three regions gets displaced over the plate. We need to first identify these regimes to quantify their range along the plate length.

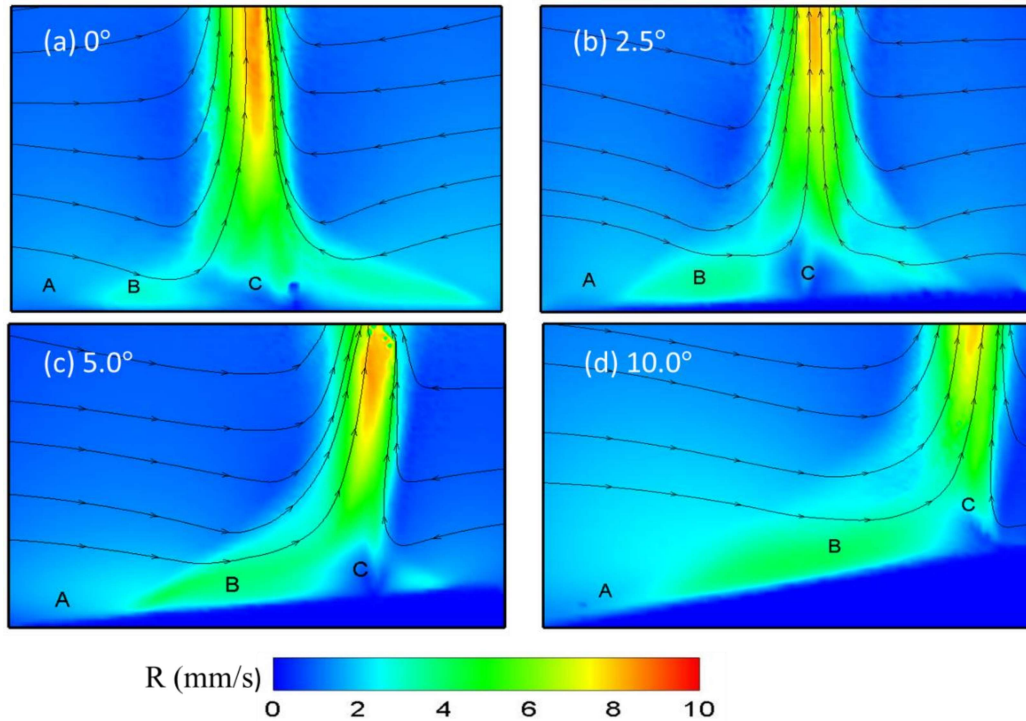


**Figure 6.4:** R-velocity contour at the angle of inclination of (a)  $0^\circ$ , (b)  $2.5^\circ$ , (c)  $5.0^\circ$  and (d)  $10.0^\circ$  for a heat flux of  $1000 \text{ W/m}^2$

### 6.3.2 Identification of various regimes

For the identification of range of these regimes, variation in hydrodynamic parameters are needed for analysis. The various criterion for determining the onset of transition were discussed in chapter 5. In this chapter, the various regimes are identified based on the variation of maximum streamwise velocity ( $u_{\max}$ ) along the length of the plate. Figure 6.5 shows the variation of  $u_{\max}$  with  $x$  for a  $2.5^\circ$  inclined plate at  $500 \text{ W/m}^2$ . The flow has been designated into three regimes: attached or laminar flow (regime A), transition (regime B) and buoyant plume (regime C) as shown in figure 6.5. It is observed from figure 6.5 that the value of  $u_{\max}$  increases along the length of the plate in both attached flow regime and transition regime. However, a more rapid increase in  $u_{\max}$  in transition regime is observed compared to attached flow regime. It is also found that the peak of the  $u_{\max}$  is obtained in the transition regime and after that  $u_{\max}$  start to decrease which indicates the entering of

fluid into the plume regime. For more clear visualization, these regimes are presented on R-velocity contour of horizontal plate at a heat flux of  $500 \text{ W/m}^2$  in figure 6.6. As can be seen from figure 6.6 that the velocity vectors are nearly parallel to each other and of small magnitude in attached flow regime. However, in the transition regime, the velocity vectors are inclined with respect to the plate indicating existence of both u-velocity and v-velocity. The magnitude of velocity is larger in transition regime as compared to attached flow regime. It is due to the fluid entrainment from both attached flow regime and the outer bulk fluid. Kitamura et al. [49] measured the temperature at the surface of a heated plate by liquid crystal thermometry. Their results showed three regimes over the plate, each with a distinct heat transfer coefficient profile. Their heat transfer coefficient values decreased from the edges towards the centre, followed by a sharp increase in the slope of the heat transfer coefficient curve followed by a gradual decrease towards a constant value at the centre of the plate. Comparison of their thermal data with the present work reveals their three regimes to be identical with those in the present work.

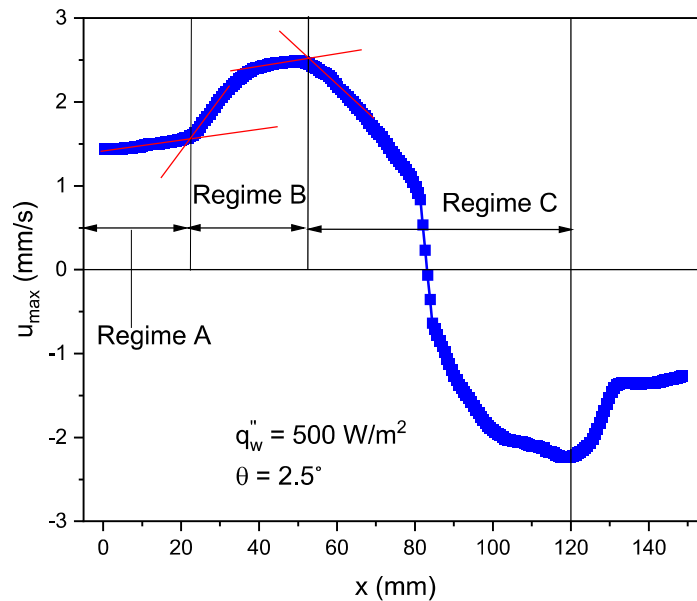


**Figure 6.5:** Identification of various flow regimes based on the variation of  $u_{\max}$  for  $2.5^\circ$  inclined plate at a heat flux of  $500 \text{ W/m}^2$

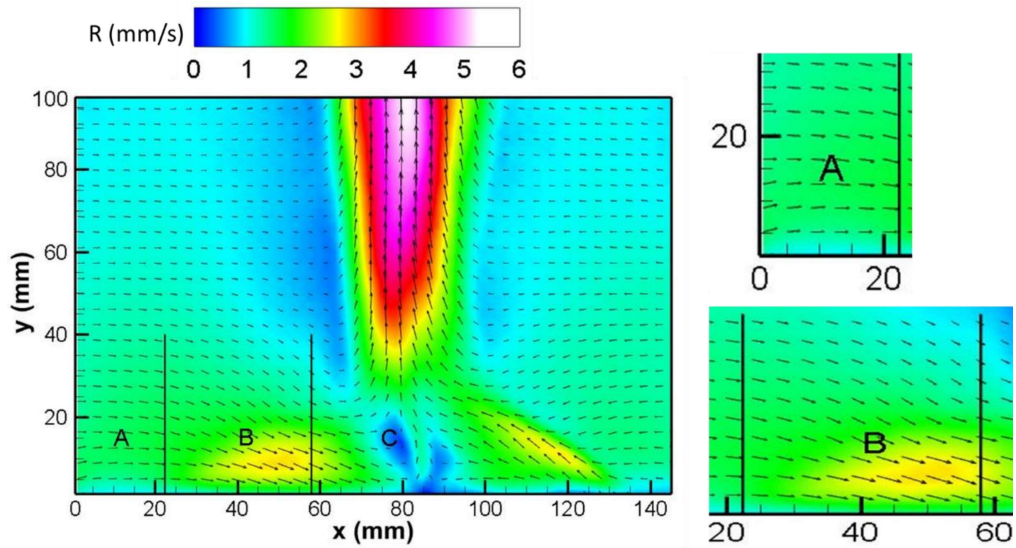


**Figure 6.6:** Various regimes show on the velocity contour for 2.5° inclined plate at 500 W/m<sup>2</sup> based on the variation of  $u_{max}$

It is observed from figure 6.5 and 6.6 that the identification criterion adopted in present work shows a decent representation of different regimes.

Figures 6.5 and 6.6 show the different characteristics features of the flow which can be divided into three regimes. The location of start of these regime and the effect of different heating and inclination angle on that location is important to consider. Now, based on the identification method discussed above, the distance of onset of transition from the leading edge ( $x_t$ ) or the attached flow regime (considered for clarity only on the left side flow regime) variation for various values of inclination angle and heating conditions is shown in figure 6.7. It can be seen that as the heat flux increases for a particular value of inclination angle, the value of  $x_t/L$  decreases i.e. transition starts earlier for a higher value of heat flux. This is because the flow tends to become thermally unstable with an increase in heat flux. It is also found from figure 6.7 that  $x_t/L$  increases with an increase of inclination angle at a particular value of heat flux. The reason is that the component of buoyancy force along the length of the plate increases with increase of plate inclination

from horizontal. Therefore, the fluid remains attached for a longer distance for a higher value of inclination angle due to a large driving potential. The maximum value of  $x_t/L$  is 0.21 and was obtained for a  $10^\circ$  inclination and  $500 \text{ W/m}^2$  heat flux.

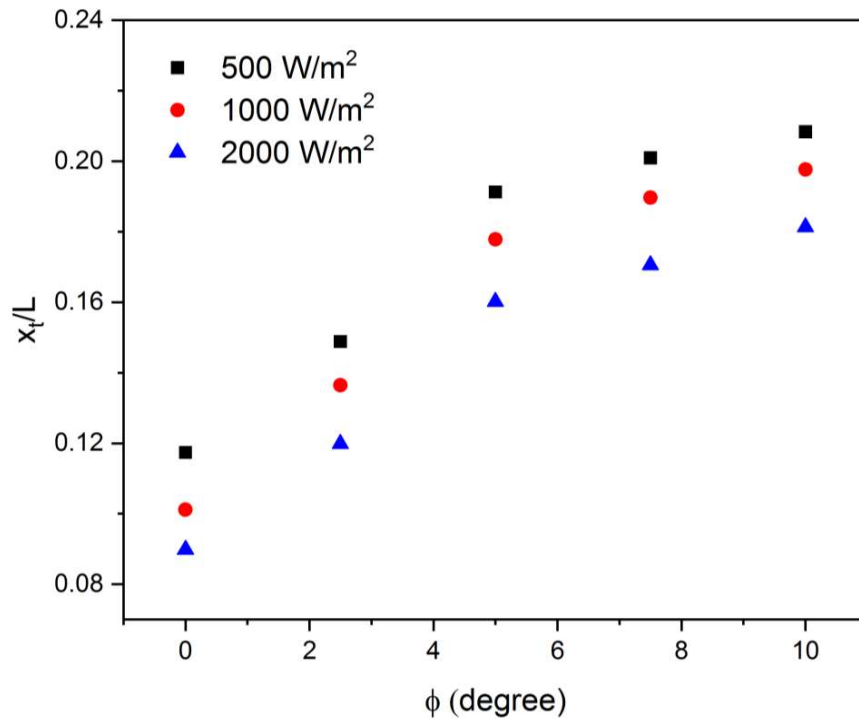


**Figure 6.7:** Onset of transition or length of attached flow regime for various values of inclination angles and heating conditions

Next, it was seen earlier that the transition regime is formed after the attached flow regime. Therefore, in figure 6.8, the length of the transition regime (obtained from left side flow regime) for various values of inclination angle and heating condition is plotted. In the present work, transition length ( $\Delta x_{tr}$ ) is the streamwise distance between the onset and end of transition (or start of plume). It is found that the transition length per unit plate length ( $\Delta x_{tr}/L$ ) increases with the heat flux and also with the inclination angle. The shifting of the buoyant plume towards trailing edge with an increase in inclination angle causes transition length to increase, as seen in figure 6.4. The value of  $\Delta x_{tr}/L$  increases from about 0.13 to

0.50 (increase of 276.25%) when the inclination angle increases from  $0^\circ$  to  $10^\circ$  for a  $500 \text{ W/m}^2$  heat flux. The maximum value of  $\Delta x_{tr}/L$  is 0.58 and it was obtained for  $10^\circ$  inclined plate at a heat flux of  $2000 \text{ W/m}^2$ . Since we have been able to identify the three different flow regimes on the basis of flow parameters, we shall now discuss in greater detail the flow behaviour over a flat horizontal plate before moving on to flow over inclined plates.

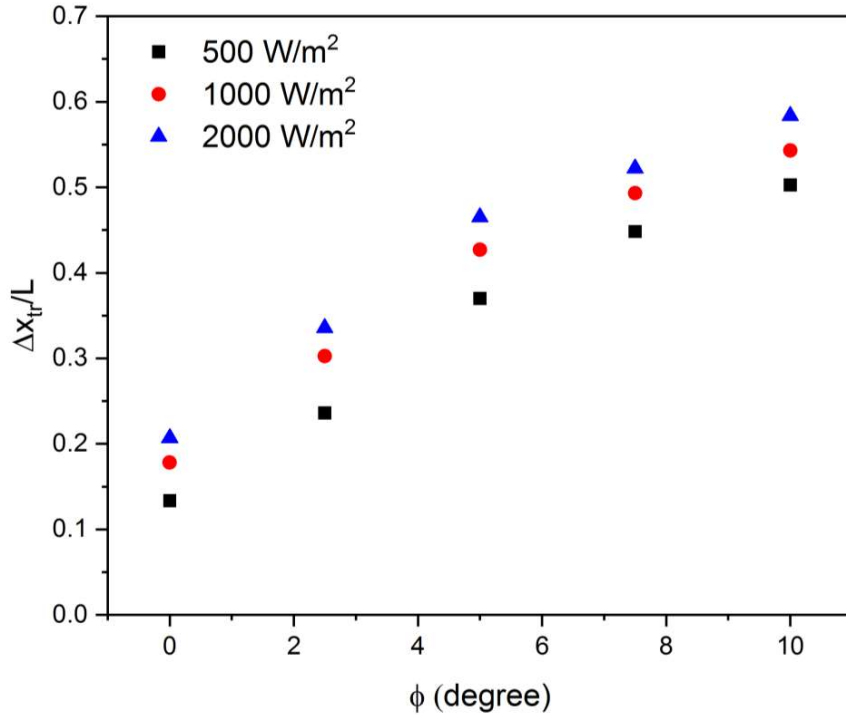


**Figure 6.8:** Length of transition regime for various values of inclination angles and heating conditions

### 6.3.3 Horizontal plate

In this section, various regimes are analysed in detail for the horizontal plate based on the variation of u-velocity and v-velocity.

#### 6.3.3.1 Variation of u-velocity

For a detailed analysis of VBL, the variation of u-velocity for horizontal plate at different heating conditions is presented in this section.

Figure 6.9 shows the u-velocity contour for a horizontal plate at a heat flux of  $500 \text{ W/m}^2$ . A symmetrical pattern is formed close to the surface about the centre of the plate. The flow velocity on both sides about the centre is nearly equal in magnitude but opposite in direction due to the fluid approaching towards the centre from the edges of the plate. This behaviour is also seen in figure 6.10 in which velocity profile is plotted on both sides of the plate at a heat flux of  $500 \text{ W/m}^2$ . The formation of a VBL can be seen from this plot. The magnitude of u-velocity in velocity profile is symmetrical about the zero u-velocity line. Above a distance of about 60 mm over the plate, the u-velocity remains constant and approaches the velocity of the outer flow for the two x-locations considered. It is also observed from figure 6.10 that the overall VBL consists of two layers: an inner VBL in which u-velocity increases from zero (no-slip condition at the wall) to a maximum value ( $u_{\max}$ ) and an outer VBL in which the u-velocity asymptotically approaches the outer fluid velocity from  $u_{\max}$ . The locus of  $u_{\max}$  in figure 6.10 shows the inner VBL thickness decreases along the length of the plate in laminar regime.

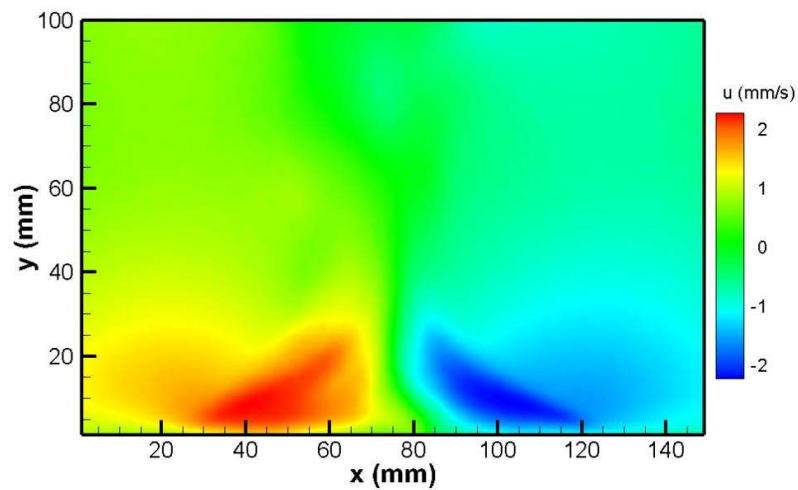


**Figure 6.9:** u-velocity contour for horizontal plate at a heat flux of  $500 \text{ W/m}^2$

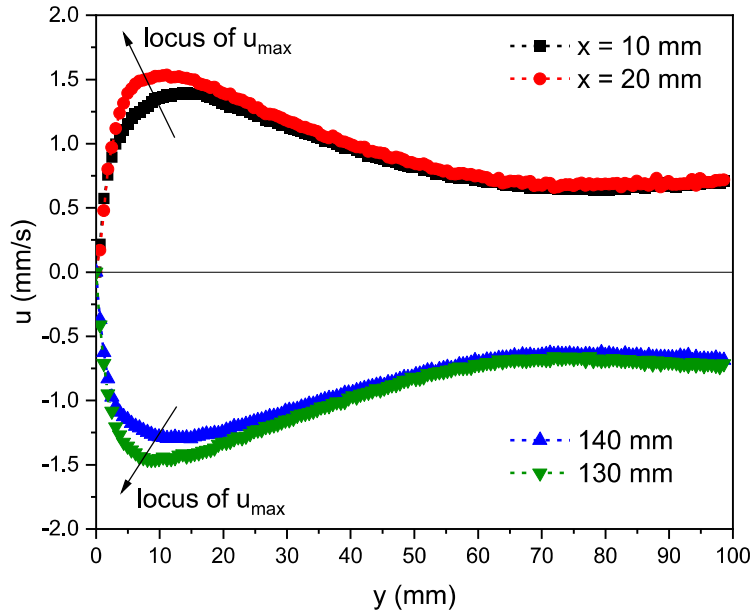


**Figure 6.10:** u-velocity profile showing the VBL formation on both side of the plate for horizontal plate at  $500 \text{ W/m}^2$  heat flux

Figure 6.11 shows the u-velocity perpendicular to the horizontal plate at a  $500 \text{ W/m}^2$  heat flux for different location along the length of the plate. It is observed that at  $x = 10 \text{ mm}$  and  $x = 20 \text{ mm}$  the velocity profile is smooth in nature. The inner VBL thickness decreases slightly when the value of  $x$  increases from 10 to 20 mm while it increases when the value of  $x$  increases from 30 to 40 mm. However, the value of  $u_{\max}$  increases while moving from  $x = 10 \text{ mm}$  to  $x = 40 \text{ mm}$ . This change in inner VBL thickness behaviour is due to the presence of two different regimes laminar and transition regime (figure 6.7 and 6.8). The typical characteristic of the VBL profile is gradually lost at  $x = 50 \text{ mm}$  and beyond. This is because  $x = 50 \text{ mm}$  and  $60 \text{ mm}$  are in the plume region where formation of VBL is distorted. It is also interesting to note that unlike the velocity profile over a vertical plate (figure 4.9 in chapter 4), the u-velocity does not approach zero at the edge of the VBL. This is because the fluid moves from the outer region towards the plate to replenish the

mass that leaves the plate in the form of a plume and as a consequence, there is a no quiescent zone. This phenomenon can be seen from the streamlines shown in figure 6.4.

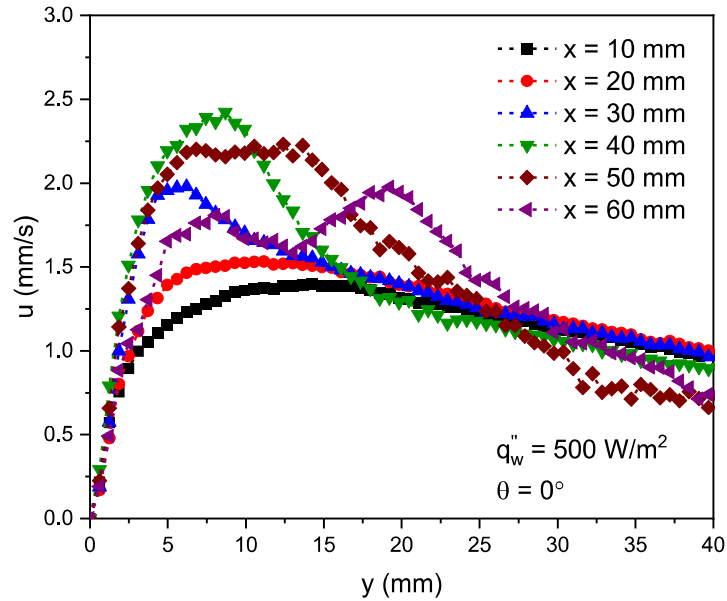


**Figure 6.11:** VBL for horizontal plate at  $500 \text{ W/m}^2$  heat flux for various values of  $x$

Figure 6.12 shows the variation of  $u$ -velocity in the streamwise direction for horizontal plate at various values of  $y$ . It can be seen that the  $u$ -velocity first gradually increases in the streamwise direction at a particular value of  $y$  in regime A. Then there is a sharp rise in its value till a maximum is reached in regime B. The tilting of streamlines towards the plate in region B in figure 6.4 indicates flow from the outer region towards the plate. This leads to a sharp increase in the  $u$  velocity in region B. After reaching a maximum value, it decreases to zero at the centre of the plate (around  $x = 75 \text{ mm}$ ) in region C. A zero  $u$  velocity indicates that the fluid lifts off vertically from the centre of the plate. Region C has therefore been denoted as the plume region. A closer examination of the velocity profile, reveals that peak value of the  $u$ -velocity first increases and then decreases with  $y$ . It is because of the VBL (figure 6.11) in which the  $u$ -velocity first increases and then

decreases with  $y$ . The  $u$ -velocity at  $y = 5$  mm shown in figure 6.12 is in the inner VBL, but it is in the outer VBL for  $y = 10$  mm and 20 mm.

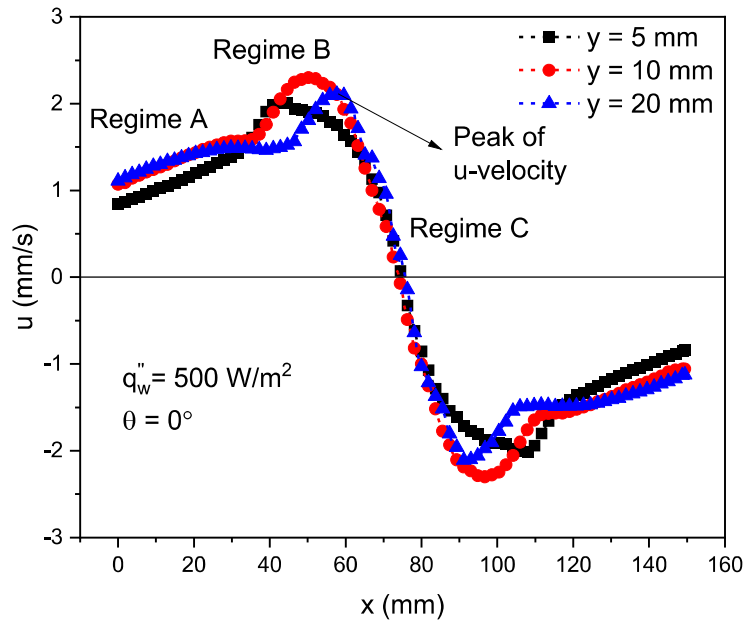


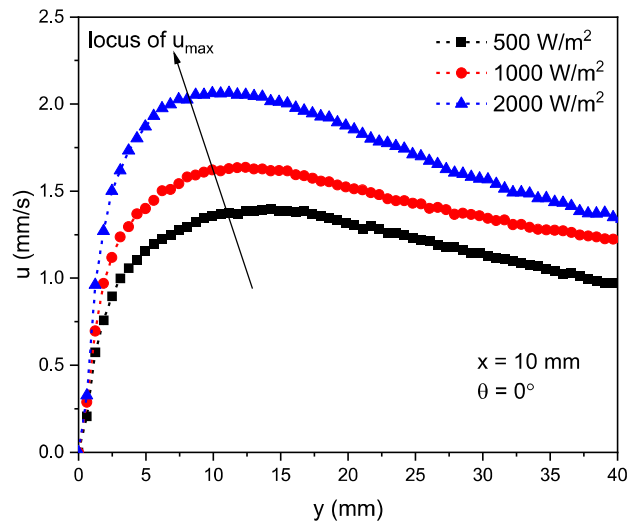
**Figure 6.12:** Variation of  $u$ -velocity in the streamwise direction for horizontal plate and for various value of  $y$  and at a heat flux of  $500 \text{ W/m}^2$

**(a). Effect of heat flux**

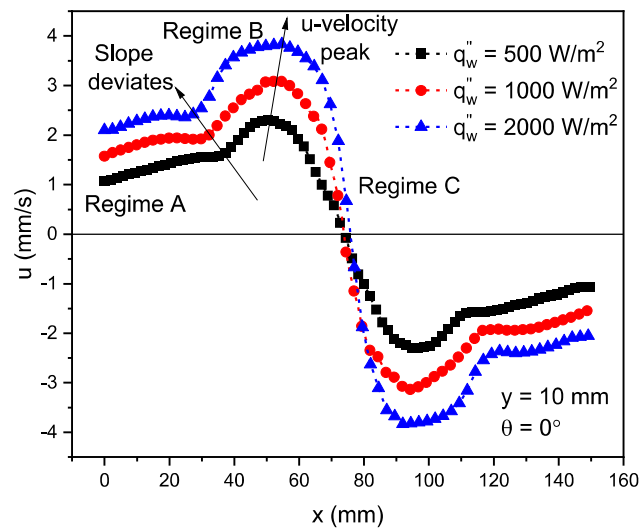
Figure 6.13 depicts the VBL for horizontal plate at different heat fluxes and at  $x = 10$  mm. It is seen that  $u$ -velocity increases with the heat flux and also peak of the velocity profile is shifted towards left of the curve. This indicates that the inner VBL thickness decreases with an increases of heat flux. It is also important to note that the  $u$ -velocity at a particular value of  $y$  in the outer VBL is higher for high heat flux value.

Figure 6.14 shows the variation of  $u$ -velocity in the streamwise direction at various values of heat fluxes for horizontal plate and at  $y = 10$  mm. As observed from figure 6.14, the slope of regime A start to deviate early in streamwise direction when heat flux increases. It indicates the early start of transition with an increase of heat flux. Also, the magnitude of  $u$ -velocity peak and its location in the streamwise direction increases with the heat flux.

For example: the  $u$ -velocity peak of 2.30 mm/s is obtained at  $x = 50.84$  mm for  $500 \text{ W/m}^2$  while its value for  $2000 \text{ W/m}^2$  is 3.83 mm/s obtained at  $x = 54.66$  mm. The earlier start of transition and a delayed occurrence of the  $u$ -velocity peak with the increase of heat flux indicates that length of the transition regime increases and laminar regime decreases as shown earlier in figures 6.7 and 6.8.



**Figure 6.13:** Velocity profile for horizontal plate at  $x = 10$  mm and for various values of heat flux



**Figure 6.14:** Variation of  $u$ -velocity in the streamwise direction for horizontal plate at various values of heat flux and at  $y = 10$  mm

### 6.3.3.2 Variation of v-velocity

For detailed analysis of buoyant plume, the variation of v-velocity for horizontal plate at different heating conditions is presented in this section.

Figure 6.15 shows the v-velocity contour for horizontal plate at a heat flux of 500 W/m<sup>2</sup>. It is observed that the magnitude of v-velocity is negligible over the plate except in the buoyant plume regime. The maximum v-velocity is at the centreline of the plume. It is also interesting to see the swaying and meandering of the plume when we move away from the plate in vertical direction. This phenomenon was recently studied by Kuehner et al. [92] for a heated cylinder placed horizontally in water using PIV technique. Due to swaying and meandering phenomenon, the mean velocity field data is plotted. The mean velocity field is calculated by averaging the experiment data collected for a period of 60 minute with a time interval of 10 minute. For better clarity, figure 6.16 is plotted by depicting the variation of v-velocity along the length of the plate at different values of y. The v-velocity profile shows the bell-shaped type of curve in which its value is almost zero in the laminar regime and maximum at near the centre of the plate. The peak of the v-velocity ( $v_{max}$ ) increases with increase in y. Also, there is a slight increase in width of the plume with y because of horizontal diffusion. The slightly negative value of v-velocity in the laminar and transition regimes can be seen because the flow from the outer layer is coming towards the plate in the downward direction (figure 6.4).

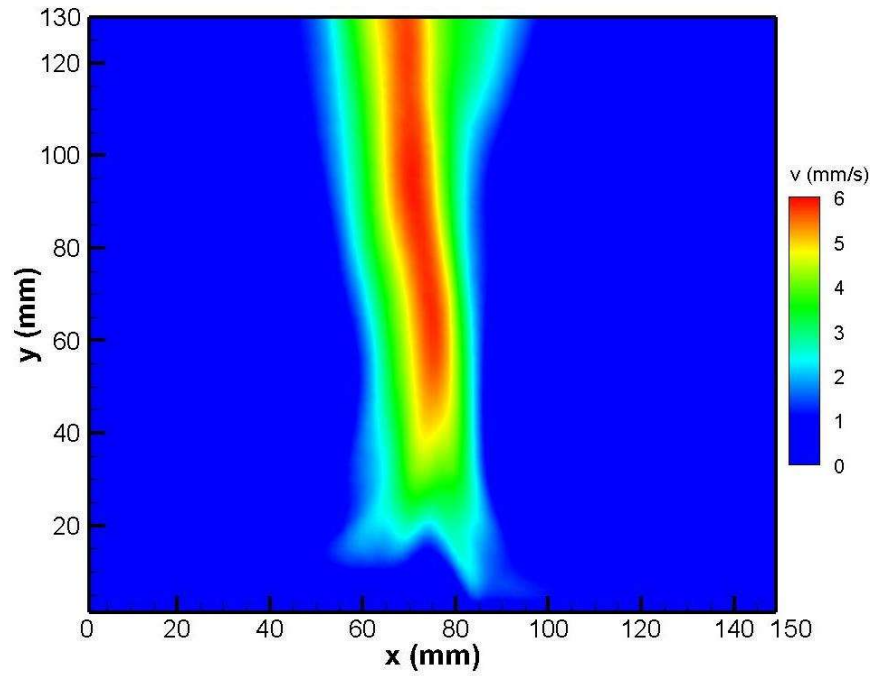


**Figure 6.15:** v-velocity contour for horizontal plate at a heat flux of  $500 \text{ W/m}^2$

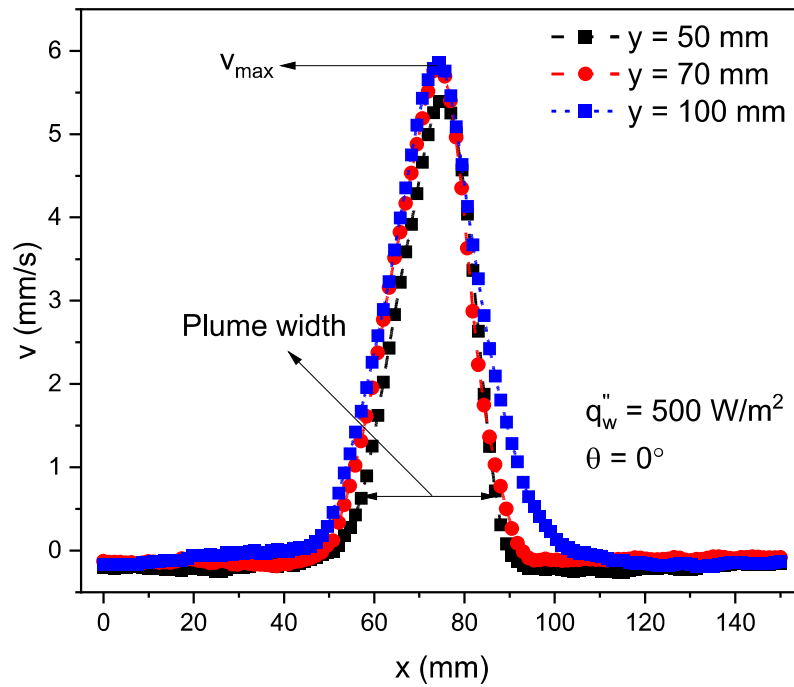


**Figure 6.16:** Variation of v-velocity with x at different values of y for a heat flux of  $500 \text{ W/m}^2$

**(a). Effect of heat flux**

The variation of  $v$ -velocity along the length of the plate at different values of heat flux is depicted in figure 6.17. Similar type of bell shaped curve is obtained at each heat flux as discussed earlier. The peak of the  $v$ -velocity increases with increase in heat flux. Also, an increase in plume width can be seen with increase in with heat flux. This behaviour can be attributed to an increase in energy available for diffusion into the bulk fluid.

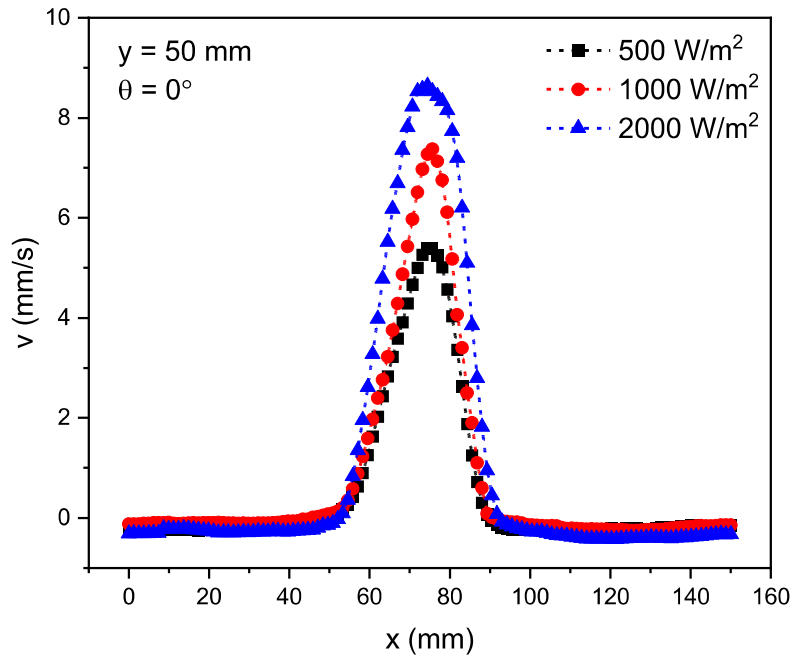


**Figure 6.17:** Variation of  $v$ -velocity with  $x$  at different values of heat flux and at  $y = 50$  mm

Figure 6.18 shows the variation of centreline velocity of the buoyant plume in vertical direction at different heat flux. An increases in  $v_{\max}$  with the heat flux at a particular value of  $y$  is seen. It is found that  $v_{\max}$  increases initially in the vertical direction for a particular heat flux but after some vertical distance, the change in  $v_{\max}$  is very small. At higher heat flux,  $v_{\max}$  starts to decrease when we move far away from the plate. For example, for  $2000 \text{ W/m}^2$  the maximum value of  $v_{\max}$  is  $10.25 \text{ mm/s}$  obtained at  $y = 79.36$

mm and after that its value decreases and at  $y = 100$  mm its value is 9.53 mm/s. It is due to the energy carried away by the plume getting diffused in a wider region.

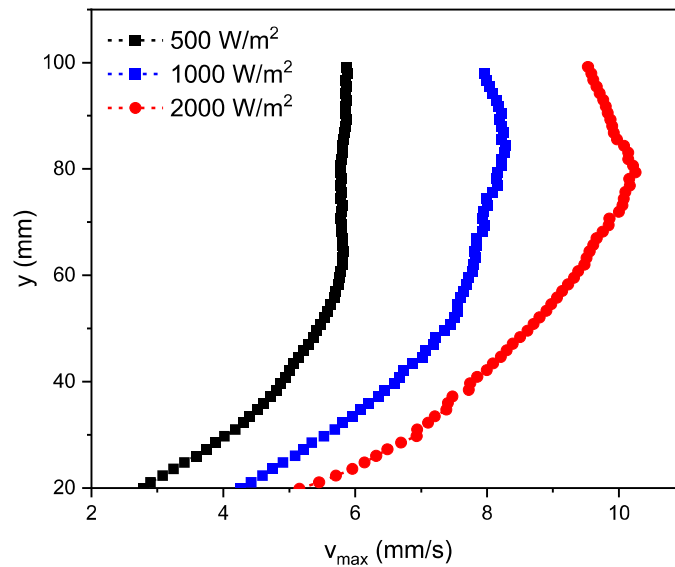


**Figure 6.18:** Variation of plume centre line velocity with  $y$  at various values of heat flux

Figure 6.19 depicts the plume width variation in the vertical direction for horizontal plate at two different heat fluxes. The plume width is defined as the distance between the locations of  $x$  where  $v$ -velocity is 10% of  $v_{\max}$ . It is observed that the plume width first decreases (due to necking) and then increases in the vertical direction (due to horizontal diffusion). It is observed earlier from figure 6.12, that for a particular value of heat flux, the peak of  $u$ -velocity shifts towards the right of the curve with increase in  $y$ . This is a signature of necking occurring close to the surface. For example, at  $500 \text{ W/m}^2$  heat flux, the plume width at  $y = 30$  mm and  $40$  mm are around  $32.97$  mm and  $30.43$  mm respectively. It is observed in figure 6.19 that an increase in heat flux causes an increase of plume width at a particular value of  $y$ . For example, at  $y = 50$  mm, the plume widths are  $29.34$  mm and  $33.62$  mm at heat fluxes of  $500 \text{ W/m}^2$  and  $2000 \text{ W/m}^2$  respectively.

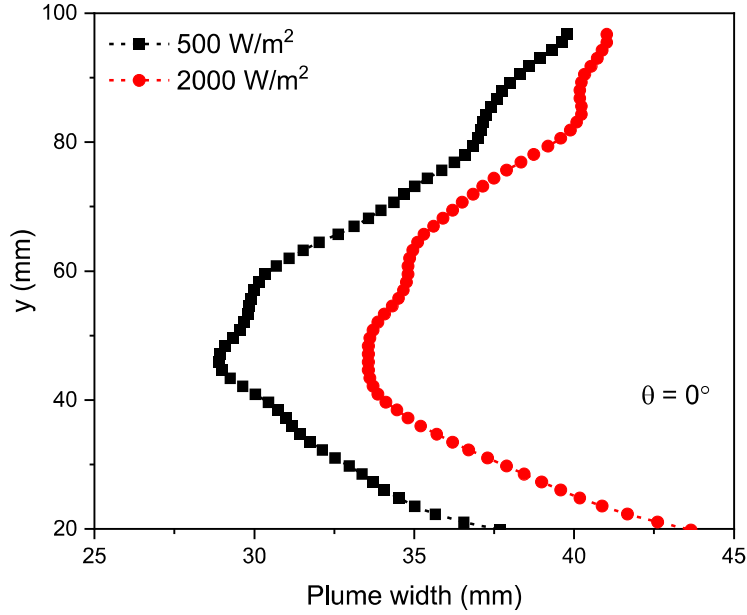


**Figure 6.19:** Variation of plume width in vertical direction at various values of heat flux

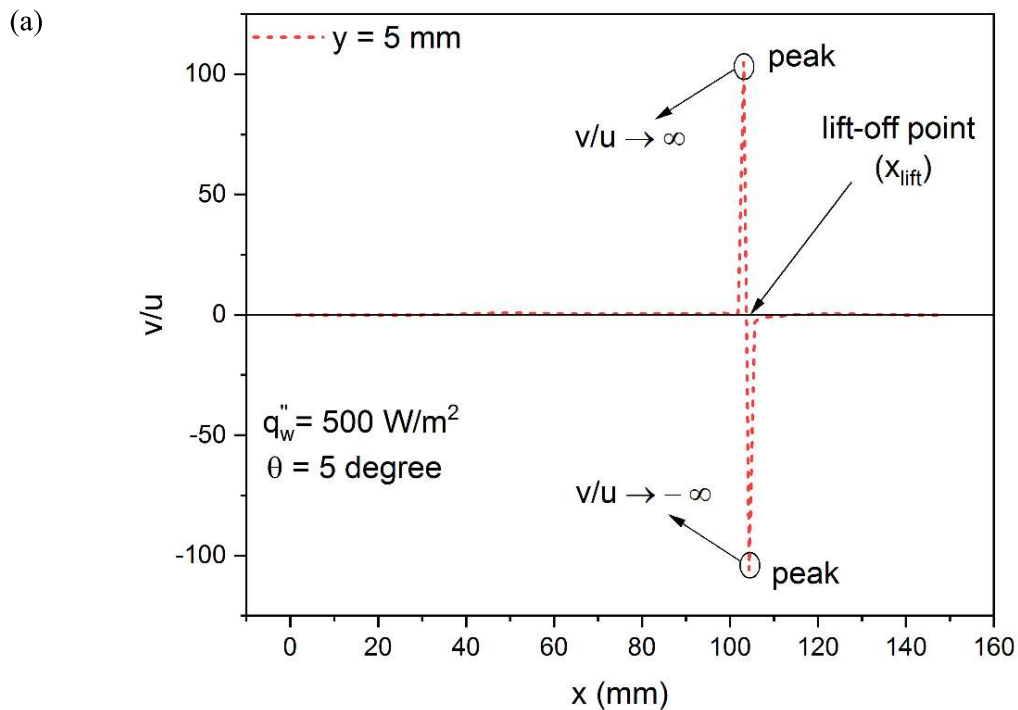
### 6.3.4 Effect of inclination on flow structures

In this section, the effect of small inclination of the plate from the horizontal on the flow behaviour is discussed.

#### 6.3.4.1 Lift-off point

In the present work, the lift-off point is designated as a location along the streamwise direction on the plate where complete conversion of horizontal component of velocity ( $u$ -velocity) into vertical component of velocity ( $v$ -velocity) takes place i.e. where the  $u$ -velocity is zero. Figure 20(a) shows the plot of  $v/u$  along  $x$  for identification of lift-off point for  $5^\circ$  inclined plate at  $500 \text{ W/m}^2$  heat flux. It can be observed from figure 20(a), that the ratio  $v/u$  is maximum near the lift off point and almost zero everywhere. The positive and negative values of  $v/u$  indicate that the entrainment of the fluid into buoyant plume takes place from both sides of the plate. So, two peaks have been observed, one where  $v/u \rightarrow \infty$  and the other where  $v/u \rightarrow -\infty$ . Therefore, the lift-off point ( $x_{\text{lift}}$ ) marked in figure 20(a), is taken as the mean values of both these location of  $x$ . Based on the above mentioned

identification method, the lift off point is calculated for all the inclination angles of the plate and heat fluxes and is shown in figure 20(b). It is observed from this figure that the  $x_{\text{lift}}/L$  increases when the inclination of the plate from the horizontal increases. Also, a negligible variation in the value of  $x_{\text{lift}}/L$  with the heat flux is observed. In light of this, it can be concluded that the lift-off point primarily depends on the inclination angle and not on the heat flux values. Similar type of observation was obtained in the experimental work of Kimura et al. [49]. They experimented with various lengths of the plate and heating conditions in water under a constant wall heat flux. The results of Kimura et al. for  $1000 \text{ W/m}^2$  and  $L = 200 \text{ mm}$  are plotted in figure 20(b) for comparison with present work. It is observed that the present experimental results are in good agreement with a maximum deviation of 6.9% obtained at a  $10^\circ$  inclination of the plate.



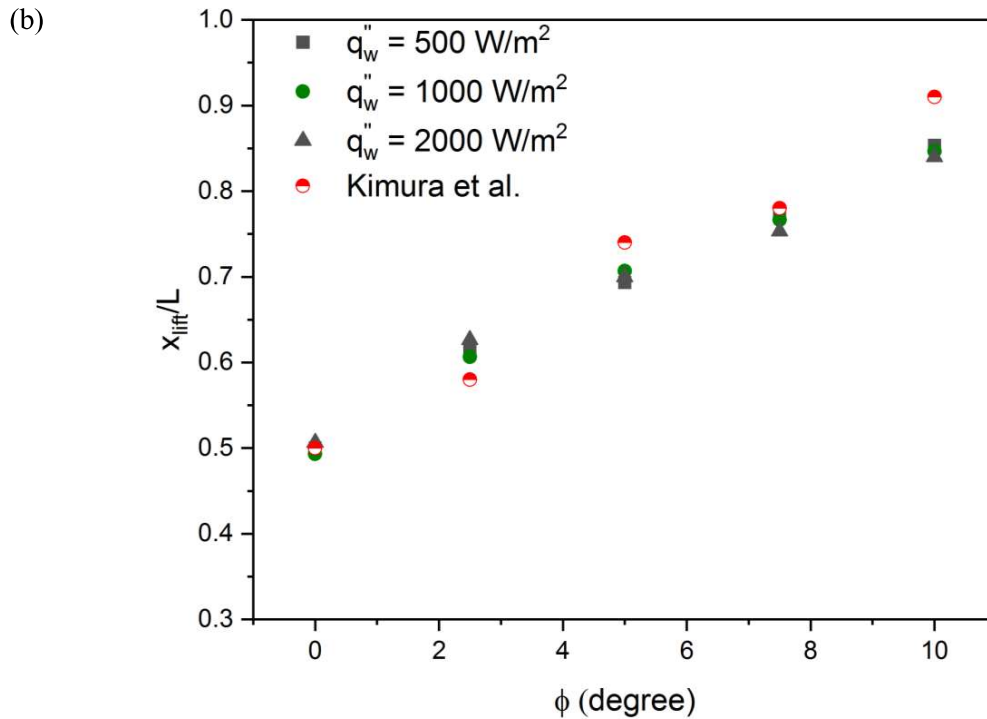


**Figure 6.20:** (a) Variation of  $v/u$  in the streamwise direction for identification of lift-off point for  $5^\circ$  inclined plate and  $500 \text{ W/m}^2$  heat flux (b) Lift-off point at different angle of inclination of the plate and heat fluxes

### 6.3.4.2 Velocity boundary layer

Figure 6.21 shows the VBL for various values of inclination angle at  $x = 10 \text{ mm}$  (laminar regime) and  $q_w'' = 1000 \text{ W/m}^2$ . It is observed that the  $u$ -velocity increases with the increase of inclination angle at a particular value of heat flux and  $y$ . The locus of the  $u_{\max}$  is seen to be shifted towards the left of the curve. This indicates the decrease of inner VBL thickness with the increase of inclination angle. For example, the  $u_{\max} = 1.64 \text{ mm/s}$  is obtained at  $y = 12.4 \text{ mm}$  for  $0^\circ$  plate inclination while for  $5^\circ$  its value is  $2.06 \text{ mm/s}$  at  $y = 8.68 \text{ mm}$ .

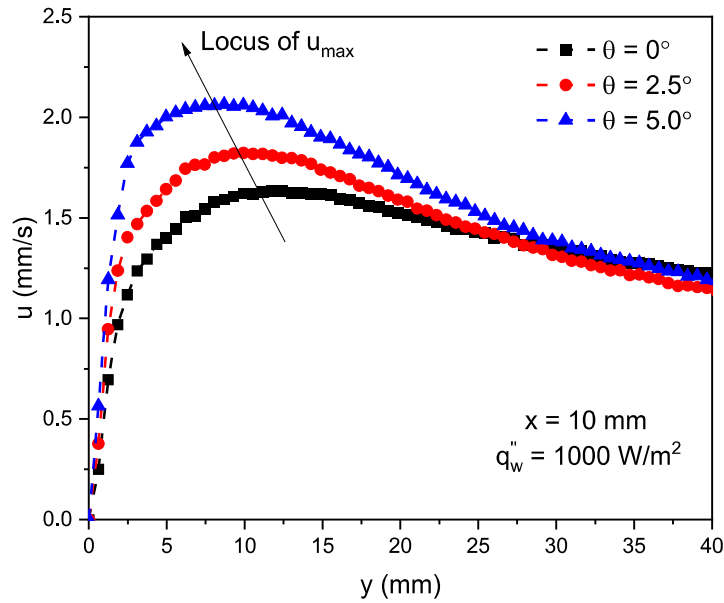


**Figure 6.21:** VBL for various values of inclination angle at  $x = 10 \text{ mm}$  and  $q_w'' = 1000 \text{ W/m}^2$

### 6.3.4.3 Buoyant plume

The variation of v-velocity with x for different inclination angles at  $y = 50 \text{ mm}$  and  $q_w'' = 1000 \text{ W/m}^2$  respectively is shown in figure 6.22. It was observed that the peak of the v-velocity ( $v_{\max}$ ) decreases with an increase in inclination angle. For example, its maximum value of  $7.74 \text{ mm/s}$  and minimum values of  $5.85 \text{ mm/s}$  are obtained for  $0^\circ$  and  $10^\circ$  plate inclinations. Additionally, the peak of the v-velocity is seen to be shifted to the right of the curve i.e. towards the plate trailing edge. This indicates the shifting of the buoyant plume towards higher end of the plate which is also seen in figure 6.4. The effect of inclination angles on the plume width (b) at a heat flux of  $500 \text{ W/m}^2$  and  $y = 50 \text{ mm}$  is presented in figure 6.23. It is seen that the value of  $b/L$  increases with the inclination of the plate at a particular value of heat flux and y. The maximum value of  $b/L$  is obtained at  $10^\circ$  inclined plate and its value is about 0.35.

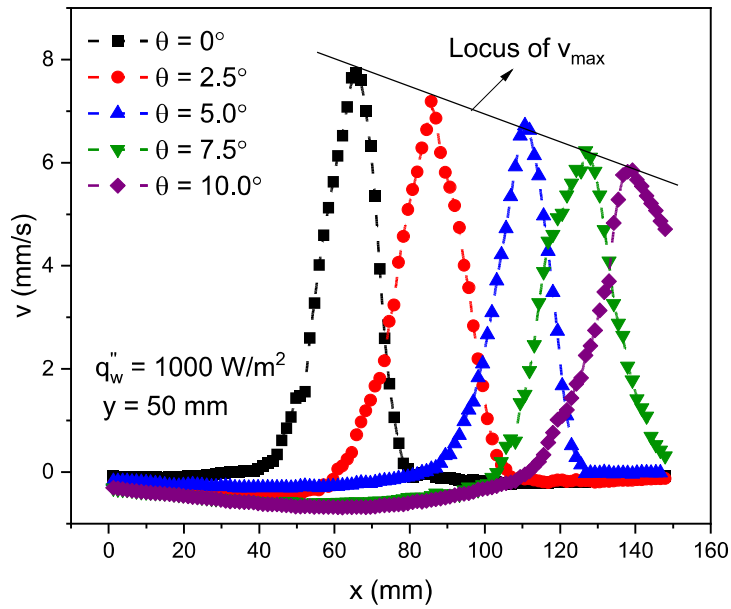


**Figure 6.22:** Variation of v-velocity in the streamwise direction at different angle of inclination of the plate for a heat flux of  $1000 \text{ W/m}^2$  and at  $y = 50 \text{ mm}$

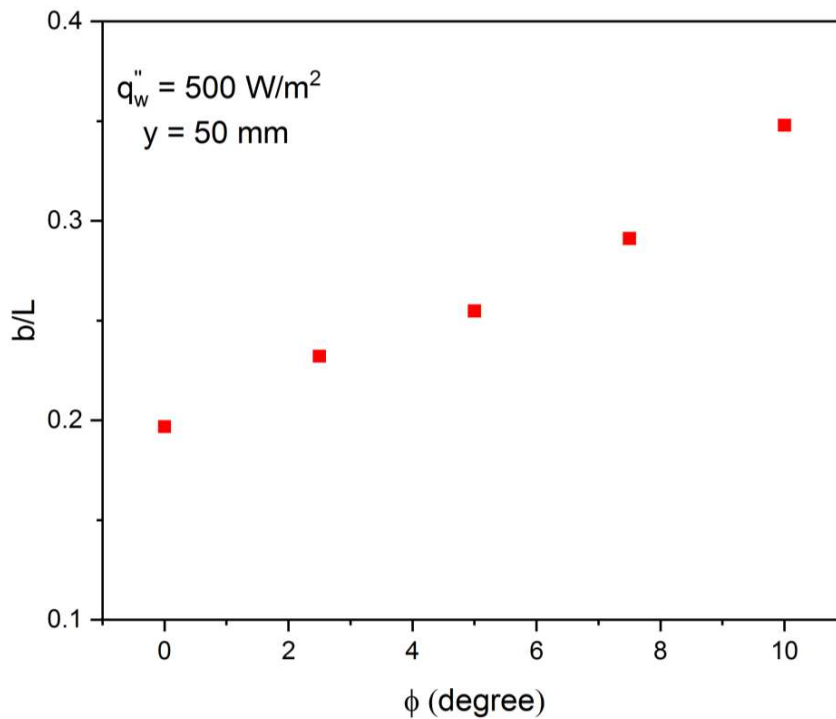


**Figure 6.23:** Variation of plume width with angle of inclination of the plate at a heat flux of  $500 \text{ W/m}^2$  and  $y = 50 \text{ mm}$

## 6.4 Conclusion

In this work, analysis of free convection fluid flow characteristics above a flat heated surface, which is horizontal and also slightly inclined to the horizontal has been carried out with the help of PIV technique. The influence of different inclinations of the plate and heat fluxes on the flow characteristics has been analysed, and its observations are as follows:

- i. As the flow moves from both sides of the plate, it is observed that at a certain distance from the both ends, the two flows interact, then separate off the plate to form a plume. This distance from the leading edge, termed as the 'lift-off' point is found to be solely determined by the inclination angles and is unaffected by the heat flux.
- ii. Based on the flow characteristics, three different regimes - attached, transition and buoyant plume regime have been identified. For the case of the horizontal plate, it is seen that in the laminar regime, the fluid close to the surface flows from both ends of the plate towards the centre. After some distance, the laminar flow gets transformed into transitional flow which is manifested by increase in boundary layer thickness and increase in u-velocity. Finally, a plume rises from the far end of the transition region. When the plates are inclined, the position of these three regions gets displaced over the plate. It is found that the onset of transition gets delayed with increasing inclination angle and occurs earlier with an increase of heat flux. The maximum value of the location of onset of transition from leading edge per unit plate length is 0.21 and was obtained for  $\phi = 10^\circ$  and  $q_w'' = 500 \text{ W/m}^2$ . On the other hand, the transition length increases with the heat flux and also with the inclination angle. The maximum value of transition length per unit plate length is 0.58 and it was obtained for  $\phi = 10^\circ$  and  $q_w'' = 2000 \text{ W/m}^2$ .
- iii. The details of VBL is discussed with help of the variation in u-velocity. It is observed from the velocity profile within the VBL, that the inner VBL thickness decreases in the

laminar regime and increases in the transition regime. Also, similar to the case of inclined plate, the inner VBL thickness decreases with the increase in inclination angle and also with the heat flux in laminar regime.

- iv. The details of the buoyant plume regime have been discussed by using the variation of v-velocity. It was found that at a particular height from the plate, the centre line velocity increases with the heat flux and decreases with the inclination angle. It is observed that plume width first decreases due to necking and then increases in the vertical direction due to horizontal diffusion. Also, an increase in heat flux and inclination angle causes an increase of plume width at a particular height from the plate.